AJNR

Neurofilament Light Chain Levels Interact with Neurodegenerative Patterns and Motor Neuron Dysfunction in Amyotrophic Lateral Sclerosis

Penelope Tilsley, Antoine Moutiez, Alexandre Brodovitch, Mohamed Mounir El Mendili, Benoit Testud, Wafaa Zaaraoui, Annie Verschueren, Shahram Attarian, Maxime Guye, José Boucraut, Aude-Marie Grapperon and Jan-Patrick Stellmann

Neurofilament Light Chain Levels Interact with Neurodegenerative Patterns and Motor Neuron Dysfunction in Amyotrophic Lateral Sclerosis

Penelope Tilsley, Antoine Moutiez, Alexandre Brodovitch, Mohamed Mounir El Mendili, Benoit Testud, Wafaa Zaaraoui, Annie Verschueren, Shahram Attarian, Maxime Guye, José Boucraut, Aude-Marie Grapperon, and Jan-Patrick Stellmann

ABSTRACT

BACKGROUND AND PURPOSE: Amyotrophic lateral sclerosis (ALS) is a neurodegenerative disease involving rapid motor neuron degeneration leading to brain, primarily precentral, atrophy. Neurofilament light chains are a robust prognostic biomarker highly specific to ALS, yet associations between neurofilament light chains and MR imaging outcomes are not well-understood. We investigated the role of neurofilament light chains as mediators among neuroradiologic assessments, precentral neurodegeneration, and disability in ALS.

MATERIALS AND METHODS: We retrospectively analyzed a prospective cohort of 29 patients with ALS (mean age, 56 [SD, 12] years; 18 men) and 36 controls (mean age, 49 [SD, 11] years; 18 men). Patients underwent 3T ($n = 19$) or 7T ($n = 10$) MR imaging, serum ($n = 23$) and CSF ($n = 15$) neurofilament light chains, and clinical ($n = 29$) and electrophysiologic ($n = 27$) assessments. The control group had equivalent 3T ($n = 25$) or 7T ($n = 11$) MR imaging. Two trained neuroradiologists performed blinded qualitative assessments of MR imaging anomalies ($n = 29$ patients, $n = 36$ controls). Associations between precentral cortical thickness and neurofilament light chains and clinical and electrophysiologic data were analyzed.

RESULTS: We observed extensive cortical thinning in patients compared with controls. MR imaging analyses showed significant associations between precentral cortical thickness and bulbar or arm impairment following distributions corresponding to the motor homunculus. Finally, uncorrected results showed positive interactions among precentral cortical thickness, serum neurofilament light chains, and electrophysiologic outcomes. Qualitative MR imaging anomalies including global atrophy ($P = .003$) and FLAIR corticospinal tract hypersignal anomalies ($P = .033$), correlated positively with serum neurofilament light chains.

CONCLUSIONS: Serum neurofilament light chains may be an important mediator between clinical symptoms and neuronal loss according to cortical thickness. Furthermore, MR imaging anomalies might have underestimated prognostic value because they seem to indicate higher serum neurofilament light chain levels.

ABBREVIATIONS: ALS = amyotrophic lateral sclerosis; ALSFRS-R = revised ALS Functional Rating Scale; CMAP = compound muscle action potential; CST = corticospinal tract; GLM = general linear model; LMN = lower motor neuron; MEP = motor-evoked potential; MNI = Montreal Neurological Institute; NfL = neurofilament light chains; TMS = transcranial magnetic stimulation; UMN = upper motor neuron

Amyotrophic lateral sclerosis (ALS) is a lethal neurodegenerative disease involving upper and lower motor neurons (UMN/LMN). Clinical manifestations initially predominate in either limb ($\sim$65%) and bulbar ($\sim$30%) or respiratory ($\sim$5%) territories, with deaths occurring anywhere from as little as a few months to up to a decade postdiagnosis, often due to respiratory failure.[1-3] Brain MR imaging is an established tool used to map and quantify regional neuronal pathology across a range of neurodegenerative diseases. In ALS, MR imaging alterations primarily occur in the motor cortex and corticospinal tract (CST).[4] In particular, the utility of conventional structural MR

imaging such as T1-weighted images in ALS has been previously demonstrated by evidencing cortical atrophy or cortical thickness loss, a hallmark of neuronal death, primarily across the motor cortex.[5] Furthermore, standard structural T2-weighted FLAIR images also show increased signal anomalies (eg, hyperintensities) at the level of the CST,[5,6] detectable both quantitatively and qualitatively through neuroradiologic assessments.[7] Despite these findings, the widespread clinical implementation of MR imaging in ALS is limited to excluding alternative diagnoses such as ALS mimics and remains to be established as a prognostic tool in ALS.[8]

The association between ALS and brain pathology as detected by MR imaging hence remains moderate and suggests the presence of yet-unknown or incompletely understood pathophysiologic mechanisms mediating this relationship. While progress is being made with more advanced mapping of clinical symptoms according to revised ALS Functional Rating Scale (ALSFRS-R) subscores,[9,10] more precise mapping of correlating biomarkers is, so far, missing. Recent advances have demonstrated that the accumulation of neurofilament light chains (NfL) in serum and CSF, an indicator of axonal damage and neural death,[11] is increased more than 9-fold in ALS compared with controls.[12] NfL seem a highly sensitive, robust biomarker for the diagnosis and prognosis of ALS,[13-15] with relatively good specificity compared with neuroinflammatory[16] and other neurodegenerative diseases.[17] NfL could thus be an informative mediator between cortical neuronal loss, observable with both qualitative neuroradiologic rating and quantitative assessment of MR images, and loss of function in ALS, visible through clinical assessments and electrophysiologic criterion standards such as transcranial magnetic stimulation (TMS), which can depict LMN/UMN dysfunction.[18,19] For example, the TMS compound muscle action potential (CMAP), a standard measure of nerve conduction, progressively decreases in ALS, reflecting LMN degeneration,[20,21] while motor-evoked-potentials (MEPs) are reduced or sometimes completely absent in ALS, reflecting UMN dysfunction and CST degradation.[18,22] The ratio between them is thought to provide more information about UMN degeneration by factoring out LMN-related biases.[23] The presence of new biologic and imaging biomarkers gives the opportunity to evaluate patients' evolution in vivo, but the link between what they mean and measure in terms of clinical, functional, and anatomic terms is still lacking.

The goal of the study was, thus, to investigate the link between qualitative neuroradiologic assessments or quantitative neurodegeneration in the precentral cortex and either serum and CSF NfL levels or clinical and electrophysiologic outcome measures in a population of patients with ALS.

MATERIALS AND METHODS

Participants

We included retrospective data from 29 patients with ALS prospectively recruited between 2013 and 2020 from the Referral Center for Neuromuscular Diseases and ALS, Marseille, France, having both MR imaging and either a serum or CSF NfL assessment. Inclusion criteria were patients who fulfilled the revised El Escorial diagnostic criteria:[24] definite ALS ($n = 5$), probable ALS ($n = 15$), probable laboratory-supported ALS ($n = 2$), and possible ALS ($n = 7$). Exclusion criteria were comorbid neurologic conditions or coexisting frontotemporal dementia, which was excluded on the basis of the *Diagnostic and Statistical Manual of Mental Illnesses*-5th edition dementia criteria and frontotemporal dementia criteria.[25] All patients were receiving medical treatment with riluzole, and most patients were right-handed, with only 2 patients having a laterality score below +40 on the Edinburgh Handedness Inventory, below the threshold for right-handedness.[26] Patients underwent clinical and electrophysiologic examinations, 3T or 7T MR imaging, and NfL assessments. Thirty-six healthy controls with an equivalent 3T or 7T MR imaging served as a control group. The inclusion criterion for control participants' data was a minimum age of 25 years, the minimum age of the ALS cohort. The study had ethics approval, and participants signed an informed consent before participating in the study.

Neurofilament Protocol

Serum and CSF NfL levels (picogram/milliliter) were measured with the R-PLEX Human Neurofilament L Antibody Set (MesoScale Discovery, F217X) according to the manufacturer's instructions.

Clinical Examination

Clinical disability was quantified using ALSFRS-R and ALSFRS-R subscores. The bulbar subscore corresponded to items 1–3 (speech, salivation, and swallowing functions); arm subscore, to items 4–6 (fine motor function: handwriting, cutting food, and dressing and hygiene); leg subscore, to items 7–9 (gross motor function: turning in bed, walking, and climbing stairs); and respiratory subscore, to items 10–12 (dyspnea, orthopnea, and respiratory insufficiency). Disease duration since symptom onset, date of diagnosis, onset site (bulbar, left leg, right leg, left arm, or right arm), and forced vital capacity were measured for all patients. The disease progression rate (ALSFRS-R slope) was also calculated on the basis of ALSFRS-R subscores sampled at 3, 6, and 12 months. Within the current article, sample size limited grouped analyses across different subgroups, such as patients with differing onset sites. The analyses presented in this article were restricted to associations across ALSFRS-R scores and subscores.

Electrophysiologic Protocol

TMS was performed using a Magstim 200 stimulator (Magstim) with a circular coil (9-cm diameter). The electromyography machine, Nicolet Viking EDX (Natus Medical) was used to record surface electromyography signals with a band-pass filter of 3–10,000 Hz and performed electrical stimulation. MEPs were recorded on both sides for the arm (abductor digiti minimi muscles) and leg (tibialis anterior muscles). MEP ratios were calculated by dividing the MEP amplitude elicited by TMS by the amplitude of the CMAP of the same muscles evoked by supramaximal electrical stimulation of the corresponding peripheral nerve (ulnar or fibular). TMS was not performed if the CMAP amplitude was <1 mV. The central motor conductance time was not measured because it cannot be measured if MEP values are too low.

MR Imaging Protocol

The 3T protocol included a 3D T1-weighted MPRAGE sequence (TR/TE/IT = 2300/2.98/900 ms, 160 sagittal slices, 1-mm^3 isotropic) and FLAIR (TR/TE/IT = 5000/395/1800 ms, 160 sagittal slices, 1-mm^3 isotropic) and was acquired using a 32-channel (32Rx/1Tx) head coil (Siemens). The 7T MR imaging protocol included a 3D T1-weighted MP2RAGE (TR/TE/TI1/TI2 = 5000/3/900/2750 ms, 256 sagittal slices, 0.6 mm^3 isotropic), FLAIR (TR/TE/IT = 8500/466/2400 ms, 192 sagittal slices, 0.8 mm^3 isotropic), and a sagittal 2D magnetization-prepared turbo FLASH B1+ mapping[27] (TR/TE = 2000/14 ms, 14 axial sections, section thickness = 5 mm, in plane resolution = 3.9 × 3.9 mm^2) and was acquired using a 32-channel (32Rx/1Tx) head coil.

Image Processing

7T MP2RAGE images were denoised.[28] 3T and 7T T1-weighted images were then skull-stripped using HD-BET (https://github.com/MIC-DKFZ/HD-BET).[29] FreeView (https://medimg.agfa.com/main/freeview-technology) was used to manually correct brain masks. FreeSurfer recon-all pipeline (https://surfer.nmr.mgh.harvard.edu/fswiki/recon-all) was used to perform surface-based analysis and estimate whole-brain cortical thickness in conjunction with mris_preproc and mri_surf2surf. Individual data were smoothed with a full width at half maximum of 10 mm and registered to the fsaverage brain.

Blinded Neuroradiologic Rating

A blinded assessment of patient and control MRIs was performed by 2 trained radiologists. The radiologists had 4 years (rater A) and 8 years (rater B) of experience. The radiologists were each given access to anonymized folders containing T1 and FLAIR images when available. Each folder contained either 3T or 7T images from 1 participant (either a control or patient). The radiologists were not informed as to the field strength of each folder or whether the folder contained control or patient images. Atrophy for the whole-brain (global), precentral, frontal, parietal, and temporal lobes was reported as "no," "mild," or "marked" for each hemisphere. The occipital lobe was used as a reference, given the relative lack of atrophy in this area in ALS. Atrophy of the precentral gyrus was reported only when very marked, given that it is the primary atrophic zone in ALS. CST atrophy was determined on the basis of the peduncles and pons. Atrophy to both was rated as "yes," only when one was "undetermined" and neither was "no."

FLAIR CST anomalies were reported using a window of 0/210 at 3T and 50/400 at 7T. MR images with substantial movement artifacts were rated as "artifacts" and removed from analyses. Any missing data were rated as "not applicable" and removed from analyses in a pair-wise fashion. Following the initial rating, the radiologists reviewed the corresponding images and provided a consensus rating when discordance occurred. Disparities were resolved by the 2 radiologists reviewing the images together and deciding which rating was the most accurate and submitting this rating as the final consensus rating. This process involved reducing ratings of CST atrophy to "yes" for atrophy to either the pons or peduncles, or "no" when no atrophy was present. This rating was used for investigating statistical associations. Participants were also grouped into those with no anomalies or at least 1 anomaly across all ratings.

Statistics

Demographic and clinical data were analyzed using R (Version 1.2.5033, packages: tidyverse [https://www.tidyverse.org/] and lmerTest [https://rdrr.io/cran/lmerTest/man/lmerTest-package.html]). Differences between control and patient characteristics and control and patient blind test ratings across raters were determined using 2-sample t tests or Wilcox t tests, depending on data normality. Associations were examined with Pearson correlations. When multiple ordered groups were present, an increase or decrease in mean values over ordered groups was analyzed with the Jonckheere-Terpstra tests, allowing, for example, detection of a trend with increasing atrophy across no-versus-mild-versus-marked atrophy groups. Any missing values marked as "not applicable" were omitted from analyses in a pair-wise fashion.

Spatial patterns of cortical thickness between patients and controls were analyzed using the surface-based general linear model (GLM) analyses (mri_glmfit and mri_glmfit-sim) of FreeSurfer. Between-patient analyses were restricted to the precentral area from the Desikan-Killiany atlas (?.aparc.annot: precentral).[30] Associations among patients' cortical thickness and ALSFRS-R subscores, MEP ratios, and serum or CSF NfL levels were also examined using GLMs. All models were adjusted for age, sex, and scanner (3T or 7T) and allowed random intercepts. An unadjusted P value below < .05 was used to explore the results. False discovery rate cluster correction was run with a P value < .05, using 1000 permutations.

RESULTS

Demographic and Clinical Data

Data from 29 patients with ALS and 36 healthy controls were analyzed. All patients participated in an MR imaging assessment, blinded assessment, and clinical assessment and had either a serum or CSF NfL assessment. Patients' data included 3T ($n = 19$) or 7T ($n = 10$) MR imaging, clinical examinations including ALSFRS-R scores ($n = 29$), electrophysiological assessments ($n = 27$), blinded assessments by 2 raters ($n = 29$), and NfL serum ($n = 23$) or CSF ($n = 15$) samples. Two patients did not have all electrophysiologic measures due to refusal to undergo certain TMS procedures and were removed from corresponding analyses, and in a further 2 patients, it was not possible to acquire MEP data for either the right arm ($n = 1$) or lower legs ($n = 1$). Within the NfL assessments, 1 patient's sample was removed from the serum NfL assessment because it was classed as an outlier, 2 patients had no serum sample, 2 patients had no CSF sample, and 15 samples were removed due to problems during the quantification process. Control data included a 3T ($n = 25$) or 7T ($n = 11$) MR imaging and blinded assessments by 2 raters ($n = 36$). As hypothesized, we observed decreased cortical thickness in patients compared with controls (Online Supplemental Data).

Patients' demographic, control group demographic and clinical details can be found in the Table. The control group had a mean age of 49 (SD, 11) years, with median and range of 51 [27–66] years, and a sex ratio of 1:1 male to female. Two-sample t tests comparing age and sex between controls and patients showed no

difference for sex ($t = 585$, $P = .34$), but a difference for age ($t = 372$, $P = .048$). Log NfL values were used for analyses due to the non-normal distribution of raw serum NfL levels according to the Shapiro-Wilk test (W statistic = 0.89, $P = .020$). The Pearson correlation showed a positive correlation between serum and CSF NfL levels ($r = 0.73$, $P = .003$), corroborating previous results in the literature showing a strong correlation between NfL in serum and CSF in ALS[31] and other diseases such as MS[32] and Parkinson disease.[33] A significant negative correlation was also observed between log serum NfL and clinical scores such as ALSFRS-R ($r = -0.63$, $P = .001$). Spearman correlations showed a significant negative correlation between log serum NfL and ALSFRS-R leg subscores ($r = -0.54$, $P = .007$), but not with ALSFRS arm subscores ($r = -0.09$, $P = .67$) or bulbar subscores ($r = -0.10$, $P = .66$). Similarly, progression rates indicated by the ALSFRS-R slope calculated across 1 year showed a significant positive correlation with log NfL serum, with quicker progression correlating with greater log serum NfL ($r = 0.48$, $P = .022$).

Neuroradiologic Rating

Radiologic assessments were performed for 36 controls and 29 patients, with a total of 1020 images rated. FLAIR scans for 9 controls and 1 patient rated as "not applicable" by radiologists were removed from corresponding analyses. One further control had imaging artifacts on CST atrophy and precentral signal and was also removed from the corresponding analyses. Concordance between the raters was 92.9% for the control hemispheres and 83.5% for patient hemispheres ($P = .036$). Global atrophy was rated "no" in 66 control and 43 patient hemispheres, "mild" in 6 control and 10 patient hemispheres, and "marked" in 0 control and 5 patient hemispheres. FLAIR anomalies were rated as "yes" in 0 control and 7 patient hemispheres and "no" in 54 control and 49 patient hemispheres. At least 1 anomaly was found in 5 controls and 24 patients. Subsequent analyses exploring the link between serum NfL and consensus ratings found higher serum NfL levels in patients with FLAIR hypersignal (W statistic = 62.5, $P = .033$) and an association with global atrophy (Jonckheere-Terpstra test = 292.5, $P = .003$; alternative hypothesis: increasing serum NfL levels with increasing anomalies) (Fig 1). Nonetheless, anomalies were

Demographic and clinical details of patients with ALS and the control cohort[a]

Variable	Central Tendency	Spread	Count (No.)
Patient cohort			
Male/female ratio	38%	[0–1]	29
Age (yr)	56	(SD, 12)	29
Duration of disease (mo)	13	[5–84]	29
Age at disease onset (yr)	55	(SD, 12)	29
Spinal: Bulbar ratio	75%	[0–1]	28
Vital capacity (%)	95%	(SD, 20)	28
Weight (kg)	69	(SD, 14)	29
ALSFRS-R (/48)	38	(SD, 5.2)	29
ALSFRS-R bulbar (/12)	12	[4–12]	29
ALSFRS-R arm (/12)	10	[3–12]	29
ALSFRS-R leg (/12)	6	[2–12]	29
ALSFRS-R slope (1 year)	0.53	[0.12–3.6]	29
MEP ratio left arm	43	[0–76]	27
MEP ratio right arm	37	[0–72]	26
MEP ratio left leg	0	[0–63]	26
MEP ratio right leg	0	[0–69]	26
Serum NfL	400	[65–1800]	23
Log serum NfL	6	(SD, 0.86)	23
CSF NfL	32,000	(SD, 19,000)	15
Log CSF NfL	10	(SD, 0.7)	15
Control cohort			
Male/female ratio	50%	[0–1]	36
Age (yr)	51	[27–66]	36

Note:— Brackets in the first Variable column refer to units (eg, months, years), or the maximum value for the given scale (eg, /12 being out of 12).

[a] Central tendency and spread are shown as mean (SD) for normally distributed data or median and [range] for non-normally distributed data. Quantitative variables are shown as percentages. The number of participants within each variable analysis is indicated in the column count.

FIG 1. Association between log serum NfL levels and anomalies based on neuroradiologic rating consensus for each hemisphere in patients with ALS. Graphs show consensus ratings compared with log serum NfL values for A, Global atrophy; B, FLAIR in CST; and C, Instances of at least 1 anomaly found on any image. Individual scatterpoints show each individual patient's data, with 2 points per patient corresponding to the consensus ratings of the left or right hemisphere and their corresponding log serum NfL value.
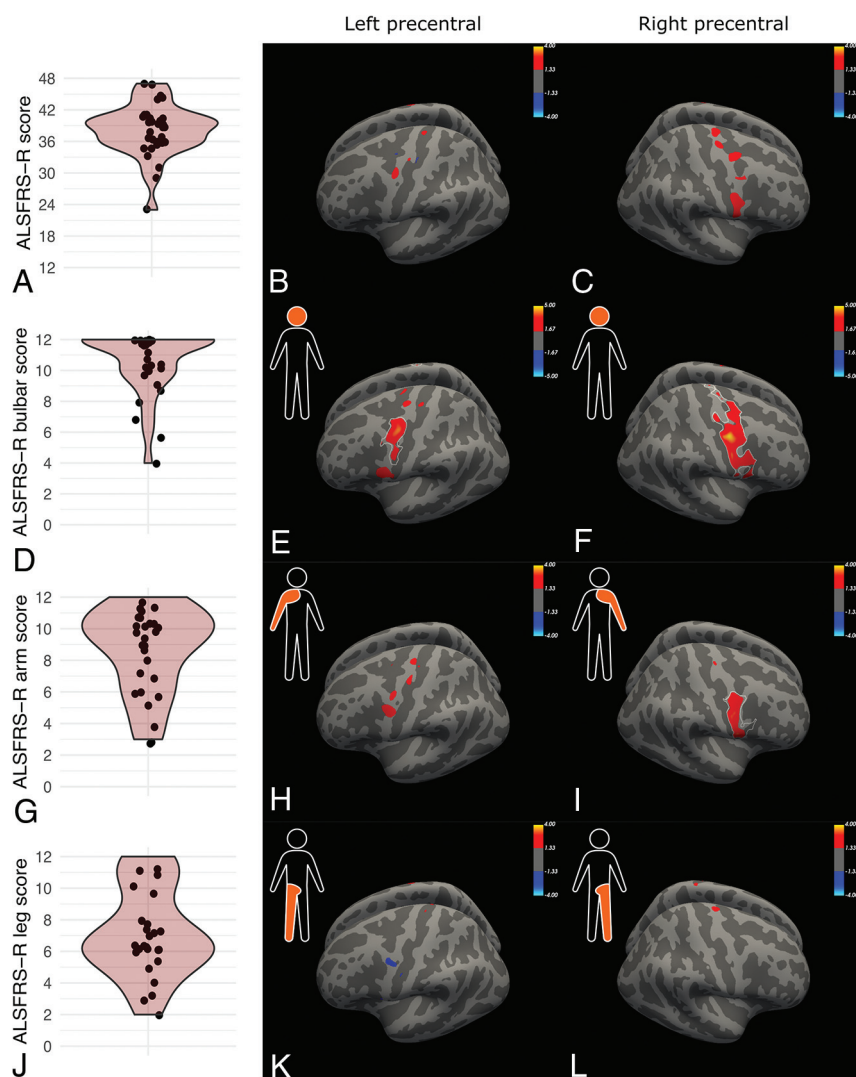
FIG 2. ALSFRS-R score and subscore distributions (*violin graphs*) and corresponding GLM comparison for patients' precentral cortical thickness and ALSFRS-R scores for *A–C*, global score. *D–F*, Bulbar. *G–I*, Arm. *J–L*, Leg region subscores. Note that while ALFSRS-R subscores are not lateralized, GLM correlations for the left precentral cortex were presumed to be related to right-limb symptoms, and vice versa for the right precentral cortex, as depicted by the *orange shading* on the silhouette. The *color scale* (signed log10 *P* values) indicates decreased cortical thickness with decreasing (less normal) ALSFRS-R scores in red (and vice versa, negative associations in blue). An uncorrected threshold of 1.3 corresponds to a log10 of *P* = .05. Significant clusters surviving cluster-wise *P* value correction (*P* < .05) are *outlined in white*.

results in expected precentral areas, we performed associations between ALSFRS-R subscores and MEP ratios. Figure 2 shows the association between ALSFRS-R scores and cortical thickness. For ALSFRS-R bulbar scores, 1 cluster in the right (precentral gyrus: size = 2395 mm^2, Montreal Neurological Institute [MNI] [x] = 44.2, MNI [y] = −9.2, MNI [z] = 45.6, *P* = .002) and left (precentral gyrus: size = 927 mm^2, MNI [x] = −45.6, MNI [y] = −9.5, MNI [z] = 50.5, *P* = .008) hemispheres survived cluster-wise correction. ALSFRS-R arm scores survived cluster-wise correction in the right hemisphere (precentral gyrus: size = 1209 mm^2, MNI [x] = 60.1, MNI [y] = 2.2, MNI [z] = 19.0, *P* = .010). Results from MEP ratios (Fig 3) showed a similar distribution, with decreased cortical thickness in the upper-leg regions of the precentral cortex being associated with decreased leg MEP ratios.

Association among NFL Levels, Electrophysiology, and Cortical Thickness

The spatial origin of NfL associated with cortical neurodegeneration is shown in Fig 4. Results showed a negative correlation between NfL levels in CSF or serum with cortical thickness (left hemisphere: $r = −0.46$, $P = .03$; right hemisphere: $r = −0.46$, $P = .03$), ie, reduced cortical thickness with increasing NfL. Furthermore, we explored the interaction between serum NfL levels and MEP ratios for each limb compared with cortical thickness in the contralateral hemisphere (Fig 5). Overall, we found positive interactions, indicating that the inverse effect of serum NfL val-

rare and serum NfL values did not differ between patients with no or at least 1 anomaly (W statistic = 51, *P* = .59). Similar statistical results were found with a simple *t* test and grouping global atrophy scores of "mild" and "marked" into a "yes" category. Furthermore, a positive association was also seen between ALSFRS-R slope, an indicator of progression rate, and global atrophy (Jonckheere-Terpstra test = 362.5, *P* value ≤ .001; alternative hypothesis: increasing across no, to mild, to marked atrophy) and FLAIR CST (W statistic = 70.5, *P* value = .034). As with previous results, no significant association was found with any anomaly (W statistic = 82, *P* = .35).

Mapping Disability Scores with Cortical Atrophy
To determine whether patterns of cortical atrophy were associated with limb-specific clinical symptoms or electrophysiologic

ues on cortical thickness is stronger (ie, the slope of the linear model is steeper) in patients with lower MEP values (higher disability). These interactions were found across arm and bulbar premotor and motor areas.

DISCUSSION
Our study investigated clinical and research grade MR imaging outcomes as bridging techniques between disability and neuronal loss in a group of patients with ALS. Serum NfL levels, currently the most promising blood biomarker in neurodegenerative diseases, served as a marker of ongoing neuronal loss and were associated with precentral area cortical thickness. While with a small sample size, uncorrected results suggest an interaction between cortical thickness and NfL with electrophysiologic outcomes, an
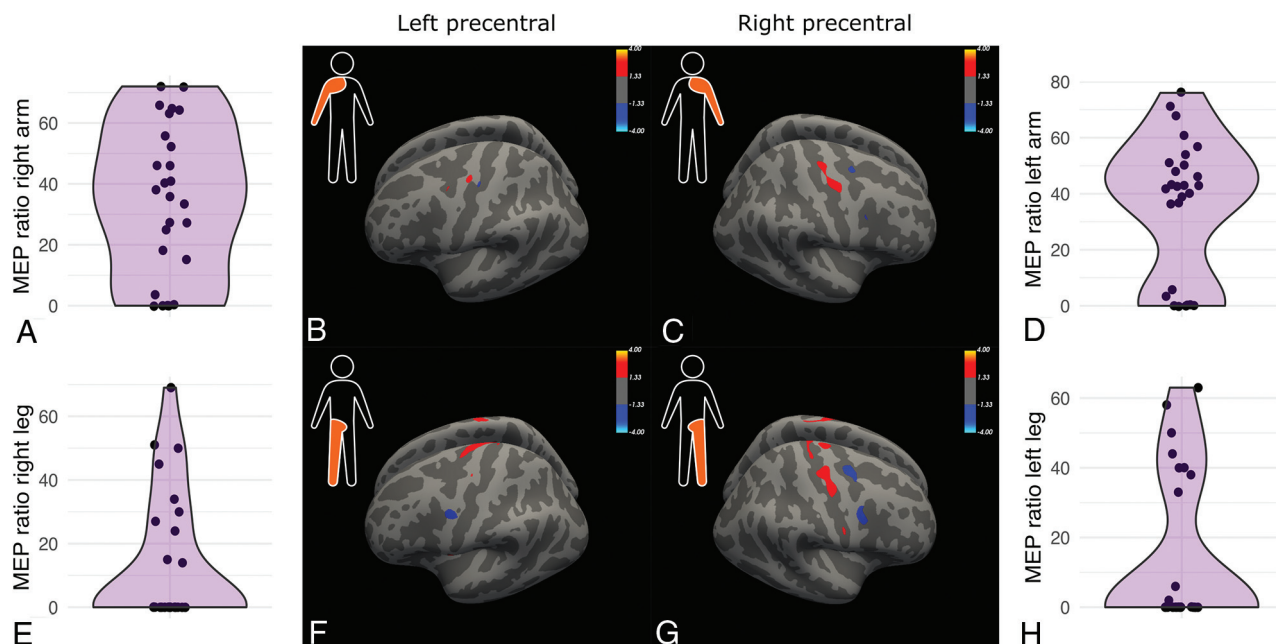
FIG 3. MEP ratio distributions (*violin plots*) across patients and corresponding GLM comparison for patients' precentral cortical thickness and electrophysiologic MEP ratios for *A* and *B*, Right arm; *C* and *D*, Left arm; *E* and *F*, Right leg; and *G* and *H*, Left leg. Correlations for the left precentral area were performed with right-limb measures, and vice versa for the right precentral area, following the *orange shading* on the silhouettes. The *color scale* (signed log10 *P* values) indicates decreased cortical thickness with decreasing (less normal) MEP ratios in red (and vice versa, negative associations in blue). Uncorrected threshold of 1.3 corresponding to a log10 of *P* = .05. Significant clusters surviving cluster-wise *P* value correction (*P* < .05) are *outlined in white*.
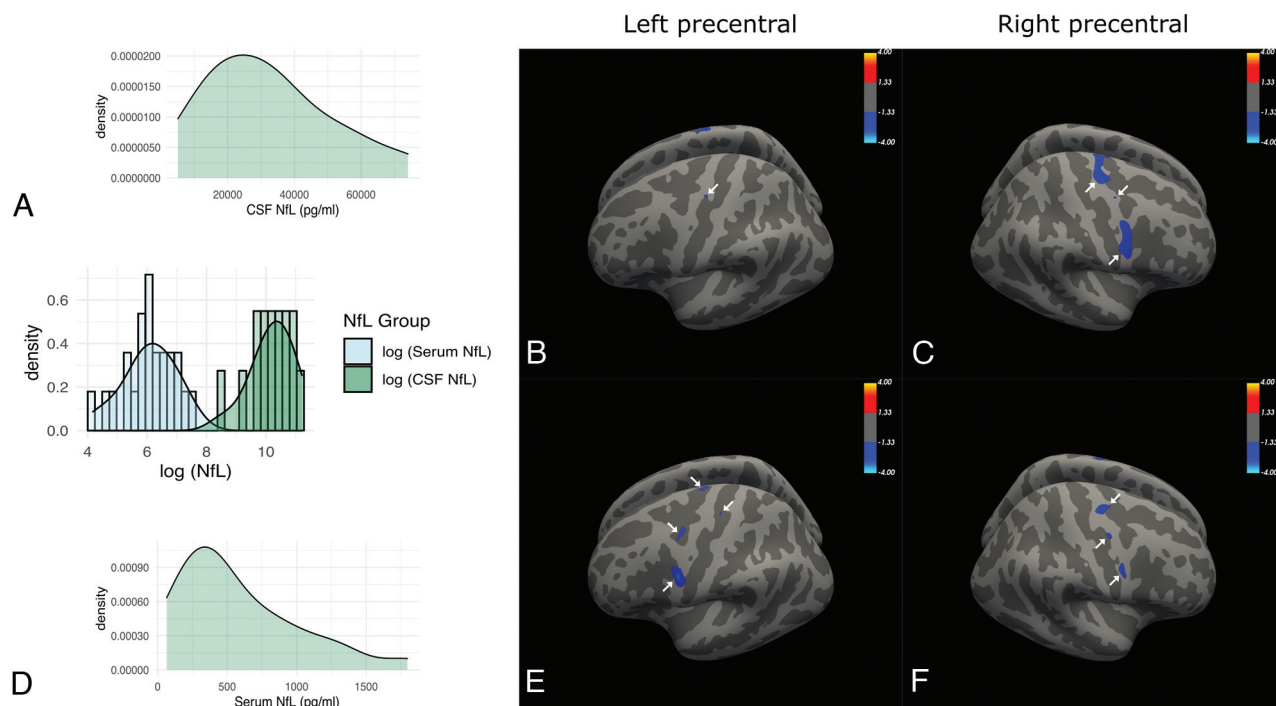
FIG 4. *A* and *D*, Distribution of CSF and serum NfL levels across patients, with corresponding log CSF and serum values represented as a combined histogram-density graph. *B* and *C*, GLM comparison for patients' precentral cortical thickness and log CSF NfL levels. *E* and *F*, GLM comparison for patients' precentral cortical thickness and log serum NfL levels. The *color scales* in *B* and *C* and *E* and *F* (signed log10 *P* values) indicate decreasing cortical thickness with increasing NfL scores in blue (and vice versa, positive associations in red). An uncorrected threshold of 1.3 corresponds to a log10 of *P* = .05. Note that the negative correlation in the left precentral area is around the premotor cortex. Significant clusters surviving cluster-wise *P* value correction (*P* < .05) are *outlined in white*.

Left precentral   **Right precentral**
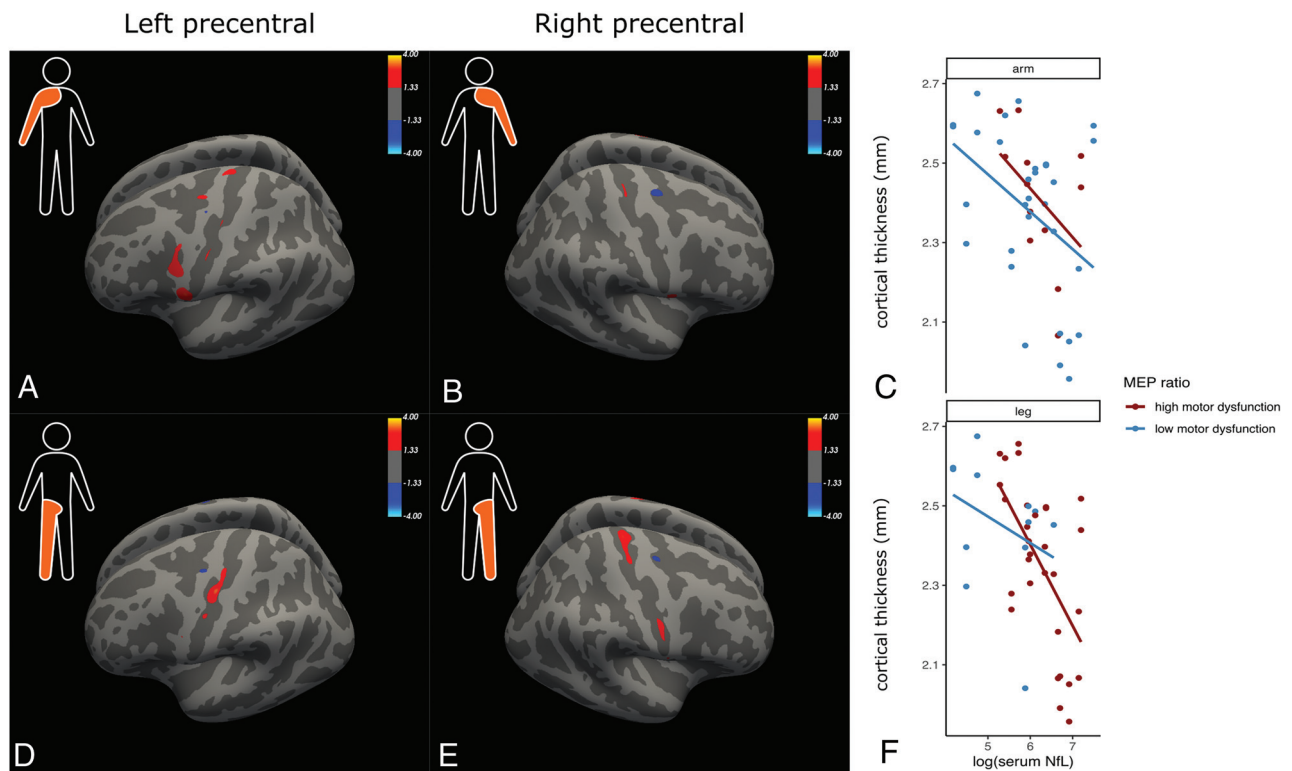
FIG 5. GLM demonstrating the interaction among patients' precentral cortical thickness, NfL levels and MEP ratios in *A*, Right arm; *B*, Left arm; *D*, Left leg; and *E*, Right leg. Panels on the right depict scatterplots and linear model estimations for the interaction between serum NfL and cortical thickness according to MEP ratios for *C*, the arm and *D*, leg split into either high motor dysfunction (low MEP ratios) or low motor dysfunction (high MEP ratios) using the mean. The *color scale* (signed log10 *P* values) where red indicates that higher MEP values were associated with a lower effect of serum NfL on cortical thickness. Uncorrected threshold of 1.3 corresponding to a log10 of *P* = .05. Significant clusters surviving cluster-wise *P* value correction (*P* < .05) are *outlined in white*.

objective measure of upper motor neuron dysfunction. Finally, despite low observations of anomalies during neuroradiologic rating, our results suggest that the visibility of FLAIR anomalies increases with higher serum NfL levels, which are linked to poorer prognosis.

Radiologic Ratings Linked to Serum Biomarkers in ALS
To date, qualitative MR imaging ratings have usually been found to be neither sensitive nor specific for the prognosis of ALS, resulting in a tendency to use clinical and electrophysiologic scores without necessarily having additional MR imaging data.[5] We investigated the link between qualitative and quantitative MR imaging and a highly specific biomarker in ALS, NfL, as well as the link to the clinical and electrophysiologic outcomes. As in other studies in ALS[31] and other diseases such as MS,[32] Parkinson disease,[33] X-linked adrenoleukodystrphy,[34] we confirmed a strong correlation between NfL in serum and CSF. In particular, serum NfL represents an easily-accessible biomarker with a much higher elevation in ALS compared with other diseases and even ALS mimics,[35] and are thought to represent axonal degeneration and death. Here, while detection of anomalies was rare, perhaps due to MR imaging being performed at the beginning of patients' disease courses, we found a meaningful association between serum NfL levels and FLAIR CST signal anomalies and global atrophy. Furthermore, we found a positive association between clinical markers for disease states and

progression with FLAIR CST and global atrophy anomalies. These results are in line with a previous study suggesting that CST hyperintensities on FLAIR images represent a marker of axonal degeneration,[6] the same pathophysiologic process thought to cause the increase in NfL.[11]

Previous studies have also demonstrated similar results, with levels of NfL shown to be positively correlated with the disease progression rate in X-linked adrenoleukodystrophy[34] and ALS,[36] while quantitative MR imaging profiles of patients with ALS vary in their disease-progression rates.[37] These results may support the prognostic value of qualitative MR imaging assessments in ALS. Larger studies with longitudinal quantitative and qualitative MR imaging data and NfL data might be necessary to clearly define the link between atrophy and NfL and could examine associations across subgroups according to the progression rate or genetic mutations, which we did not address in our study. Additionally, our study focused on precentral areas, yet changes in subcortical and extramotor structures, the most frequent longitudinal changes in ALS,[38] or spinal cord atrophy could warrant exploration. It has already been demonstrated, for instance, that the rate of serum NfL change is associated with brain volume changes across several widespread brain areas in frontotemporal dementia, a similar disease thought to be on the same spectrum, with NfL levels able to capture rates of brain atrophy for certain mutation carriers.[39]

Spatial Distribution of ALS Symptoms

We demonstrated that the association between precentral cortical thinning and limb ALSFRS-R subscores and MEP ratios followed a distribution generally respecting the motor homunculus. As with previous results, the spatial distribution was observed bilaterally,[4,6] and associations were prominent for bulbar scores.[9,10] We also observed overlap of subscores into other motor homunculus regions. One explanation could be the nonspecific nature of ALSFRS-R subscores,[40,41] yet we also observed overlap for MEP ratios. Alternatively, studies have suggested apparent spreading of symptoms to adjacent motor regions.[6,9] Our results may thus be in line with recent challenges to the somewhat misinterpreted strict segmentation of the homunculus across sensorimotor areas,[42] with increasing suggestions of a more distributed, overlapping profile, particularly among body regions with higher physical proximity.[43,44]

Interaction between Motor Dysfunction and NfL

Finally, while results did not survive cluster correction, likely due to small sample size, uncorrected results for cortical thickness, MEPs, and NfL showed an overall positive interaction, with a negative association between cortical thickness and serum NfL levels that was stronger in patients with decreased MEP ratios. This result could be interpreted as demonstrating axonal loss primarily at the level of motor cortex neurons or CST. Reduced MEPs, or higher disability, is observed in patients with axonal loss across the motor cortex, while NfL levels reflect a more global axonal loss. Serum NfL may thus be a useful marker of ongoing neurodegeneration, which is associated with cortical atrophy and electrophysiologic measures of motor neuron function. A longitudinal study in patients with ALS showed that serum NfL levels indicated CST degeneration.[31] Furthermore, NfL increase even before symptoms are present, and remain stable and elevated throughout the disease course.[45] Here, we extend arguments for multimodal assessments in ALS[41] by presenting the opportunity to combine noninvasive markers of neurodegeneration and muscle function. It has already been shown, for example, from other cross-sectional studies that the combination of noninvasive measures from DTI and electrophysiology could represent a useful biomarker in ALS during initial disease phases,[46] while, examination of iron abnormalities from susceptibility weighted images represented a marker of UMN degeneration based on ALSFRS-R clinical scores.[6] Further studies with larger sample sizes and longitudinal evolutions of these markers alongside CST degradation or quantitative DTI would be essential in fully detailing the link among NfL, symptoms, and neurodegeneration to create standardized maps of cortical degradation in disease states.[47,48]

Limitations

Our main limitation was reduced power due to a small data set. While we used pair-wise deletion which maximized the amount of data within each analysis, certain measures such as CSF NfL were more heavily impacted by missing values, which reduced our ability to examine associations. Given the strong correlations between serum NfL and CSF NfL, correlations based on the larger serum NfL sample aimed to reduce the potential impact on this article. Ultimately a larger study with serum and CSF NfL data

could examine more deeply the links and differences between these 2 measures in terms of atrophy and clinical outcomes. We also used 3T and 7T MR imaging data, which have differing sensitivities to anomalies and cortical thickness when spatial resolution differs.[49] The use of identical, standardized surface-based postprocessing using FreeSurfer and inclusion of an MR imaging scanner as a covariate in statistical analyses aimed to reduce the associated potential bias.

Within the blinded rating assessment, complete anonymization across participant groups (control or patient) and field strength (3T or 7T) also aimed to reduce similar biases. Performing analyses on a subset of the data without 7T images did not significantly change the presented results. Furthermore, due to the low levels of patients with bulbar onset ($n = 6$), our cohort was largely patients with spinal onset with higher leg disability according to ALSFRS-R subscores and MEP ratios. Ultimately, this feature could have impacted the current results. Additionally, NfL may also be linked to neurodegeneration within the spinal cord, which we did not explore. Finally, while age was incorporated into statistical analyses, FLAIR anomalies and global atrophy become more apparent with age, even in healthy controls. The blinded rating assessments may thus have been influenced by age.

CONCLUSIONS

Our study evidenced the benefit of using radiologic qualitative and quantitative MR imaging assessment of cortical thickness in ALS, alongside noninvasive markers such as serum NfL and clinical and electrophysiologic evaluations for a detailed mapping of ongoing neurodegeneration. While quantitative MR imaging measures have been increasingly promoted, particularly in the context of multimodal assessment of ALS, whether qualitative assessments are able to reflect the same link between neurodegeneration and clinical outcomes has been less demonstrated. Here we provide preliminary evidence toward the link between NfL and both quantitative and qualitative measures to improve our understanding of ALS pathophysiology and extend arguments promoting multimodal standardized approaches in advancing the prognostic capabilities of these methods.

REFERENCES

1. Hardiman O, Al-Chalabi A, Chio A, et al. **Amyotrophic lateral sclerosis.** *Nat Rev Dis Primers* 2017;3:17071–79 CrossRef Medline
2. Grad LI, Rouleau GA, Ravits J, et al. **Clinical spectrum of amyotrophic lateral sclerosis (ALS).** *Cold Spring Harb Perspect Med* 2017;7: a024117 CrossRef Medline
3. Kiernan MC, Vucic S, Cheah BC, et al. **Amyotrophic lateral sclerosis.** *Lancet* 2011;377:942–55 CrossRef Medline
4. Thorns J, Jansma H, Peschel T, et al. **Extent of cortical involvement in amyotrophic lateral sclerosis: an analysis based on cortical thickness.** *BMC Neurol* 2013;13:148 CrossRef Medline
5. Mazón M, Costa JF, Ten-Esteve A, et al. **Imaging biomarkers for the diagnosis and prognosis of neurodegenerative diseases: the example of amyotrophic lateral sclerosis.** *Front Neurosci* 2018;12:784 CrossRef Medline
6. Vázquez-Costa JF, Mazón M, Carreres-Polo J, et al. **Brain signal intensity changes as biomarkers in amyotrophic lateral sclerosis.** *Acta Neurol Scand* 2018;137:262–71 CrossRef Medline

7. Schweitzer AD, Liu T, Gupta A, et al. **Quantitative susceptibility mapping of the motor cortex in amyotrophic lateral sclerosis and primary lateral sclerosis.** *AJR Am J Roentgenol* 2015;204:1086–92 CrossRef Medline

8. Verstraete E, Turner MR, Grosskreutz J, et al; attendees of the 4th NiSALS meeting. **Mind the gap: the mismatch between clinical and imaging metrics in ALS.** *Amyotroph Lateral Scler Frontotemporal Degener* 2015;16:524–29 CrossRef Medline

9. Jin J, Hu F, Zhang Q, et al. **Dominant heterogeneity of upper and lower motor neuron degeneration to motor manifestation of involved region in amyotrophic lateral sclerosis.** *Sci Rep* 2019;9:20059 CrossRef Medline

10. Schuster C, Kasper E, Machts J, et al. **Focal thinning of the motor cortex mirrors clinical features of amyotrophic lateral sclerosis and their phenotypes: a neuroimaging study.** *J Neurol* 2013;260:2856–64 CrossRef Medline

11. Khalil M, Teunissen CE, Otto M, et al. **Neurofilaments as biomarkers in neurological disorders.** *Nat Rev Neurol* 2018;14:577–89 CrossRef Medline

12. Forgrave LM, Ma M, Best JR, et al. **The diagnostic performance of neurofilament light chain in CSF and blood for Alzheimer's disease, frontotemporal dementia, and amyotrophic lateral sclerosis: a systematic review and meta-analysis.** *Alzheimers Dement (Amst)* 2019;11:730–43 CrossRef Medline

13. Gaiani A, Martinelli I, Bello L, et al. **Diagnostic and prognostic biomarkers in amyotrophic lateral sclerosis: neurofilament light chain levels in definite subtypes of disease.** *JAMA Neurol* 2017;74:525–32 CrossRef Medline

14. Rossi D, Volanti P, Brambilla L, et al. **CSF neurofilament proteins as diagnostic and prognostic biomarkers for amyotrophic lateral sclerosis.** *J Neurol* 2018;265:510–21 CrossRef Medline

15. Benatar M, Wuu J, Turner MR. **Neurofilament light chain in drug development for amyotrophic lateral sclerosis: a critical appraisal.** *Brain* 2022;146:2711–16 CrossRef Medline

16. Brodovitch A, Boucraut J, Delmont E, et al. **Combination of serum and CSF neurofilament-light and neuroinflammatory biomarkers to evaluate ALS.** *Sci Rep* 2021;11:703 CrossRef Medline

17. Verde F, Steinacker P, Weishaupt JH, et al. **Neurofilament light chain in serum for the diagnosis of amyotrophic lateral sclerosis.** *J Neurol Neurosurg Psychiatry* 2019;90:157–64 CrossRef Medline

18. Grapperon AM, Verschueren A, Jouve E, et al. **Assessing the upper motor neuron in amyotrophic lateral sclerosis using the triple stimulation technique: a multicenter prospective study.** *Clin Neurophysiol* 2021;132:2551–57 CrossRef Medline

19. Geevasinga N, van den Bos M, Menon P, et al. **Utility of transcranial magnetic simulation in studying upper motor neuron dysfunction in amyotrophic lateral sclerosis.** *Brain Sci* 2021;11:906 CrossRef Medline

20. de Carvalho M, Swash M. **Lower motor neuron dysfunction in ALS.** *Clin Neurophysiol* 2016;127:2670–81 CrossRef Medline

21. Rutkove SB. **Clinical measures of disease progression in amyotrophic lateral sclerosis.** *Neurotherapeutics* 2015;12:384–93 CrossRef Medline

22. Vucic S, Stanley Chen KH, Kiernan MC, et al. **The clinical diagnostic utility of transcranial magnetic stimulation: report of an IFCN committee.** *Clin Neurophysiol* 2008;150:131–75 CrossRef Medline

23. de Carvalho M, Chio A, Dengler R, et al. **Neurophysiological measures in amyotrophic lateral sclerosis: markers of progression in clinical trials.** *Amyotroph Lateral Scler Other Motor Neuron Disord* 2005;6:17–28 CrossRef Medline

24. Brooks BR, Miller RG, Swash M, et al; World Federation of Neurology Research Group on Motor Neuron Diseases. **El Escorial revisited: revised criteria for the diagnosis of amyotrophic lateral sclerosis.** *Amyotroph Lateral Scler Other Motor Neuron Disord* 2000;1:293–99 CrossRef Medline

25. Rascovsky K, Hodges JR, Knopman D, et al. **Sensitivity of revised diagnostic criteria for the behavioural variant of frontotemporal dementia.** *Brain* 2011;134:2456–77 CrossRef Medline

26. Oldfield RC. **The assessment and analysis of handedness: the Edinburgh inventory.** *Neuropsychologia* 1971;9:97–113 CrossRef Medline

27. Fautz H, Vogel M, Gross P, et al. **B1 mapping of coil arrays for parallel transmission.** In: *Proceedings of the International Society for Magnetic Resonance in Medicine.* May 3–9, 2008;1247. Toronto, Ontario, Canada

28. O'Brien KR, Kober T, Hagmann P, et al. **Robust T1-weighted structural brain imaging and morphometry at 7T using MP2RAGE.** *PLoS One* 2014;9:e99676 CrossRef Medline

29. Isensee F, Schell M, Pflueger I, et al. **Automated brain extraction of multisequence MRI using artificial neural networks.** *Hum Brain Mapp* 2019;40:4952–64 CrossRef Medline

30. Desikan RS, Ségonne F, Fischl B, et al. **An automated labeling system for subdividing the human cerebral cortex on MRI scans into gyral based regions of interest.** *Neuroimage* 2006;31:968–80 CrossRef Medline

31. Menke RAL, Gray E, Lu CH, et al. **CSF neurofilament light chain reflects corticospinal tract degeneration in ALS.** *Ann Clin Transl Neurol* 2015;2:748–55 CrossRef Medline

32. Piehl F, Kockum I, Khademi M, et al. **Plasma neurofilament light chain levels in patients with MS switching from injectable therapies to fingolimod.** *Mult Scler* 2018;24:1046–54 CrossRef Medline

33. Hansson O, Janelidze S, Hall S, et al; Swedish BioFINDER study. **Blood-based NfL: a biomarker for differential diagnosis of parkinsonian disorder.** *Neurology* 2017;88:930–37 CrossRef Medline

34. Weinhofer I, Rommer P, Zierfuss B, et al. **Neurofilament light chain as a potential biomarker for monitoring neurodegeneration in X-linked adrenoleukodystrophy.** *Nat Commun* 2021;12:1816 PMC] CrossRef Medline

35. Gille B, De Schaepdryver M, Goossens J, et al. **Serum neurofilament light chain levels as a marker of upper motor neuron degeneration in patients with amyotrophic lateral sclerosis.** *Neuropathol Appl Neurobiol* 2019;45:291–304 CrossRef Medline

36. Vacchiano V, Mastrangelo A, Zenesini C, et al. **Plasma and CSF neurofilament light chain in amyotrophic lateral sclerosis: a cross-sectional and longitudinal study.** *Front Aging Neurosci* 2021;13:753242 CrossRef Medline

37. El Mendili MM, Verschueren A, Ranjeva JP, et al. **Association between brain and upper cervical spinal cord atrophy assessed by MRI and disease aggressiveness in amyotrophic lateral sclerosis.** *Neuroradiology* 2023;65:1395–403 CrossRef Medline

38. Menke RA, Körner S, Filippini N, et al. **Widespread grey matter pathology dominates the longitudinal cerebral MRI and clinical landscape of amyotrophic lateral sclerosis.** *Brain* 2014;137:2546–55 CrossRef Medline

39. van der Ende EL, Meeter LH, Poos JM, et al; Genetic Frontotemporal dementia Initiative (GENFI). **Serum neurofilament light chain in genetic frontotemporal dementia: a longitudinal, multicentre cohort study.** *Lancet Neurol* 2019;18:1103–11 CrossRef Medline

40. Bede P, Bokde A, Elamin M, et al. **Grey matter correlates of clinical variables in amyotrophic lateral sclerosis (ALS): a neuroimaging study of ALS motor phenotype heterogeneity and cortical focality.** *J Neurol Neurosurg Psychiatry* 2013;84:766–73 CrossRef Medline

41. Wirth AM, Khomenko A, Baldaranov D, et al. **Combinatory biomarker use of cortical thickness, MUNIX, and ALSFRS-R at baseline and in longitudinal courses of individual patients with amyotrophic lateral sclerosis.** *Front Neurol* 2018;9:614 CrossRef Medline

42. Catani M. **A little man of some importance.** *Brain* 2017;140:3055–61 CrossRef Medline

43. Muret D, Root V, Kieliba P, et al. **Beyond body maps: Information content of specific body parts is distributed across the somatosensory homunculus.** *Cell Rep* 2022;38:110523 CrossRef Medline

44. Schellekens W, Bakker C, Ramsey NF, et al. **Moving in on human motor cortex: characterizing the relationship between body parts with non-rigid population response fields.** *PLoS Comput Biol* 2022;18:e1009955 CrossRef Medline

45. Bergman J, Dring A, Zetterberg H, et al. **Neurofilament light in CSF and serum is a sensitive marker for axonal white matter injury in MS.** *Neurol Neuroimmunol Neuroinflamm* 2016;3:e271 CrossRef Medline

46. Geraldo AF, Pereira J, Nunes P, et al. **Beyond fractional anisotropy in amyotrophic lateral sclerosis: the value of mean, axial, and radial diffusivity and its correlation with electrophysiological conductivity changes.** *Neuroradiology* 2018;60:505–15 CrossRef Medline

47. Wagner J, Weber B, Urbach H, et al. **Morphometric MRI analysis improves detection of focal cortical dysplasia type II.** *Brain* 2011;134:2844–54 CrossRef Medline

48. Wang ZI, Alexopoulos AV, Jones SE, et al. **Linking MRI postprocessing with magnetic source imaging in MRI-negative epilepsy.** *Ann Neurol* 2014;75:759–70 CrossRef Medline

49. Lüsebrink F, Wollrab A, Speck O. **Cortical thickness determination of the human brain using high resolution 3T and 7T MRI data.** *Neuroimage* 2013;70:122–31 CrossRef Medline